

*ovalis*: Functional response, handling time and exploitation of individual *Ceratium* cells. *J. Plankton Res.* **6**: 1131–1144.

TURLEY, C. M., R. C. NEWELL, AND D. B. ROBINS. 1986. Survival strategies of two small marine ciliates and their role in regulating bacterial community structure under experimental conditions. *Mar. Ecol. Prog. Ser.* **33**: 59–70.

ZEHNDER, A., AND P. R. GORHAM. 1960. Factors influencing the growth of *Microcystis aeruginosa*. *Can. J. Microbiol.* **6**: 645–660.

Received: 30 June 1999  
Accepted: 31 January 2000  
Amended: 6 March 2000

*Limnol. Oceanogr.*, 45(5), 2000, 1180–1186  
© 2000, by the American Society of Limnology and Oceanography, Inc.

## Mass transfer versus kinetic control of uptake across solid-water boundaries

**Abstract**—We present general nondimensional solutions for uptake across a solid-water boundary, considering the combined influences of mass transfer flux limitation and uptake reaction kinetics. Mass transfer processes are represented by a general mass transfer velocity. Reaction kinetics are represented by first-order and Monod models. Mathematical solutions are well approximated by standard mass transfer models for low values of the derived nondimensional mass transfer velocity and by standard kinetic models for high values. Approximate limiting values of the nondimensional mass transfer velocity are defined for mass transfer control and kinetic control. The intermediate region, where both mass transfer and kinetics influence the solution, is relatively broad for first-order kinetics and Monod kinetics in oligotrophic environments. Both limits decrease as concentration increases in the Monod solution, such that under increasingly eutrophic conditions mass transfer control becomes less important, the intermediate range shrinks, and kinetic control becomes an increasingly good approximation. Example calculations using data from experimental ecosystems indicate that boundary nutrient uptake was mass transfer controlled or intermediate under oligotrophic conditions. Nutrient pulses applied to the systems caused temporary eutrophication, which resulted in temporary kinetic control.

Uptake of nutrients and dissolved gases across solid-water boundaries is an important part of biogeochemical cycling in natural aquatic ecosystems (Pasciak and Gavis 1974; Boudreau and Guinasso 1982; Jorgensen and Revsbech 1985; Riber and Wetzel 1987; Santschi et al. 1990; Koch 1994). Uptake is affected both by mass transfer across the thin layer of fluid adjacent to the boundary and by reaction kinetics at or below the boundary. Uptake tends to be mass transfer controlled when reaction rates are faster than mass transfer rates (Boudreau and Guinasso 1982; Santschi et al. 1991; Thomas and Atkinson 1997). Conversely, uptake tends to be kinetically controlled when mass transfer rates are faster than reaction rates. The relative influences of these two factors have been studied for many different aquatic processes, including diagenesis and dissolution at the sea floor (Boudreau and Guinasso 1982; Santschi et al. 1990), uptake of nutrients by phytoplankton (Pasciak and Gavis 1974), uptake of phosphorus by periphyton (Riber and Wetzel 1987), fixation of carbon at leaf surfaces (Wheeler 1980; Koch 1994), and uptake of nutrients by coral reefs (Patterson et al. 1991; Atkinson and Bilger 1992).

Previous investigators have used several experimental methods for determining whether a reaction is taking place under mass transfer control or kinetic control. Frank-Kamenetskii (1969) advocated estimating the maximum possible mass transfer rate and comparing it to the observed uptake rate. If the observed uptake rate is lower than the maximum mass transfer rate, then uptake is either intermediate between the two extremes or kinetically controlled. If the observed uptake rate is equal to the maximum mass transfer rate, then uptake is mass transfer controlled. Another technique is to measure uptake rate under different flow conditions. If observed uptake rate increases with increased turbulence or mixing, then uptake is either mass transfer controlled or intermediate (Koch 1994; Thomas and Atkinson 1997). Riber and Wetzel (1987) used yet another method in which experiments were performed with the same flow but with varying amounts of biomass at the interface. Because no change in overall flux was observed, they concluded that the process was mass transfer controlled.

These experimental techniques are useful for estimating the influence of mass transfer processes on uptake, but they have two inherent problems. First, they require extensive experimentation to achieve even baseline characterizations. Second, none of these techniques can distinguish the relative degree of mass transfer control versus kinetic control. In particular, it is difficult to distinguish experimentally between the intermediate range, where both mass transfer and kinetics are important, and true mass transfer control or kinetic control.

Another technique that has been applied to the problem is mathematical modeling, assuming a steady state balance in which the uptake rate is equal to the mass transfer rate (Frank-Kamenetskii 1969). Mathematical models of this balance may be distinguished by both the physical configuration of the problem of interest and the choice of kinetic model. Frank-Kamenetskii (1969) and Boudreau and Guinasso (1982) equated expressions for mass transfer across flat boundaries to first-order reaction kinetics. Bilger and Atkinson (1995) equated expressions for mass transfer in coral reef communities to first-order kinetics. Pasciak and Gavis (1974) considered mass transfer to phytoplankton cells with Monod uptake kinetics. Boudreau and Scott (1978) formulated an expression for mass transfer to manganese nodules with Monod kinetics. Wheeler (1980) considered mass transfer to giant kelp leaves with Monod uptake kinetics. Ploug

et al. (1999) explored mass transfer to phytoplankton colonies in turbulent flows with Monod kinetics.

These modeling studies are significant contributions to our understanding of the factors that influence the balance between mass transfer control and kinetic control, but they have had two general limitations. First, they have tended to concentrate on specific problems and have not addressed the issue in general. This is especially true of the Monod kinetics solutions; Monod kinetics are more applicable than first-order kinetics for many ecological uptake processes, but the solutions are considerably more complex and hence less amenable to general exploration. Second, they have tended to concentrate on the asymptotic behaviors of the solutions (pure mass transfer control or kinetic control) without considering the intermediate range in much detail and frequently without specifying quantitative limits of validity for the asymptotic solutions.

This note addresses both of these limitations. We generalize the problem by expressing it in terms of a nonspecific mass transfer velocity; we reduce the number of variables through the use of appropriate dimensionless ratios; we derive dimensionless full solutions for both the first-order and Monod cases; and we compare and contrast the two cases. We also identify values of these dimensionless ratios that serve as approximate limits of validity for kinetic and mass transfer control. We conclude by presenting example calculations for the walls and benthos of experimental ecosystems and discussing implications for mass transfer control of boundary nutrient uptake in different environments.

*Background*—In general, mass transfer is expressed mathematically as

$$F = \beta(C_\infty - C_o), \quad (1)$$

where  $F$  is flux ( $\text{M L}^{-2} \text{T}^{-1}$ ),  $\beta$  is the mass transfer velocity ( $\text{L T}^{-1}$ ),  $C_\infty$  is the bulk fluid concentration away from the boundary in ( $\text{M L}^{-3}$ ), and  $C_o$  is the concentration at the boundary ( $\text{M L}^{-3}$ ).  $\beta$  is strongly dependent on the configuration of the system under consideration. Perhaps the most straightforward configuration is flow over a hydrodynamically smooth, flat surface, such as the muddy deep ocean floor (Santschi et al. 1991; Dade 1993), where a diffusive sublayer just above the boundary plays the role of a mass transfer limiting stagnant film. Under these conditions,  $\beta$  may be estimated as

$$\beta = 0.1Sc^{-2/3}u_* \quad (2)$$

(e.g., Dade 1993), where  $Sc = \nu/D$  is the Schmidt number,  $\nu$  is the kinematic viscosity ( $\text{L}^2 \text{T}^{-1}$ ),  $D$  is the molecular diffusivity ( $\text{L}^2 \text{T}^{-1}$ ),  $u_* = (\tau_b/\rho)^{0.5}$  is the shear velocity ( $\text{L T}^{-1}$ ),  $\tau_b$  is the bottom shear stress ( $\text{F L}^{-2}$ ), and  $\rho$  is the density of water ( $\text{M L}^{-3}$ ). Other, more complicated expressions may be derived for flow over leaf surfaces (Wheeler 1980), flow around sinking phytoplankton cells (Pasciak and Gavis 1974), phytoplankton colonies in turbulent flows (Ploug et al. 1999), flow over individual corals (Patterson 1992), flow over coral communities (Thomas and Atkinson 1997; Baird and Atkinson 1997), etc. More complex system configurations often necessitate semiempirical expressions for  $\beta$ , but in general it depends on flow speed, heat flux (if any), the

length scale(s) of interest,  $\nu$ , and  $D$  (Frank-Kamenetskii 1969). Many recent investigations of  $\beta$  express it in terms of dimensionless Sherwood ( $Sh$ ) or Stanton ( $St$ ) numbers, which are themselves expressed in terms of dimensionless Reynolds numbers ( $Re$ ) and  $Sc$  (e.g., Patterson 1992; Thomas and Atkinson 1997; Ploug et al. 1999). As in the present development, nondimensionalization of the problem consolidates both experiments and analyses.

Uptake kinetics at a solid-water boundary may be represented mathematically in several different forms. The simplest form for uptake that depends on concentration but does not saturate at high concentrations is the first-order expression

$$R = kC_o, \quad (3)$$

where  $R$  is the reaction rate ( $\text{M L}^{-2} \text{T}^{-1}$ ) and  $k$  is a reaction rate constant ( $\text{L T}^{-1}$ ). First-order kinetics have been used to describe reactions such as decay of organic carbon in oxygenated environments (Fogler 1992) and the uptake of nutrients by coral communities (Bilger and Atkinson 1995). Michaelis-Menten or Monod kinetics represent an alternative ecologically important reaction model for growth or uptake rates that become saturated at some high concentration (e.g., Atkinson and Davies 1974). Monod kinetics are written

$$R = \frac{V_m C_o}{K_m + C_o} \quad (4)$$

where  $V_m$  is the maximum uptake rate and  $K_m$  is the concentration at which the uptake rate is one-half of its maximum.

The solution for the steady state uptake rate is derived by equating the mass transfer rate (Eq. 1) to the uptake rate (Eq. 3 or Eq. 4). The first-order model is obtained by setting Eq. 3 equal to Eq. 1,

$$R = kC_o = \beta(C_\infty - C_o). \quad (5)$$

The Monod model is obtained by setting Eq. 4 equal to Eq. 1,

$$R = \frac{V_m C_o}{K_m + C_o} = \beta(C_\infty - C_o) \quad (6)$$

The solutions to both these models are straightforward, though the Monod case is more complex than the first-order case. In fact, they have both been derived by others as described above. However, analysis of the solutions is complicated by the number of variables involved, and comparison of the solutions is further complicated by the fact that some of the variables are different. Both of these issues may be addressed by expressing and solving Eqs. 5 and 6 in terms of appropriate, comparable dimensionless ratios.

*Dimensionless solutions*—The first-order case is almost trivial, but it provides an instructive introduction to the Monod case. Dividing Eq. 5 by  $kC_\infty$  yields

$$\frac{R}{kC_\infty} = \frac{C_o}{C_\infty} = \frac{\beta}{k} \left( 1 - \frac{C_o}{C_\infty} \right) \quad (7)$$

and using the right-hand equality of Eq. 7 to eliminate  $C_o/C_\infty$  yields

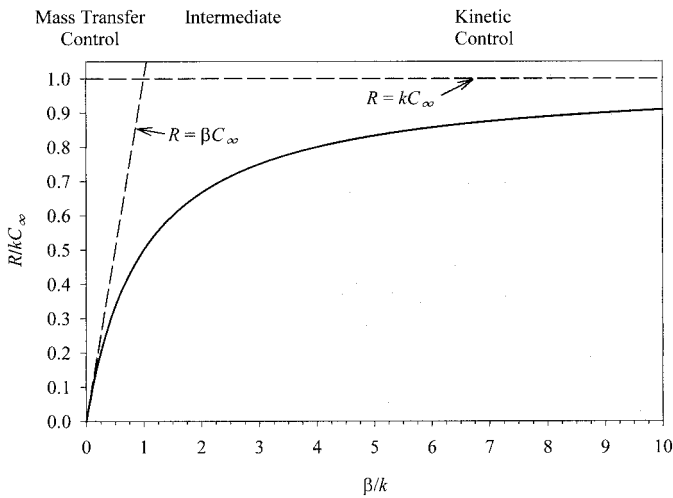


Fig. 1. Solid line—dimensionless uptake rate  $R/kC_\infty$  plotted against dimensionless mass transfer coefficient  $\beta/k$  for first-order kinetics (Eq. 8). Dashed line on left—Mass transfer control approximation  $R = \beta C_\infty$ . Dashed horizontal line—Kinetic control approximation  $R = kC_\infty$ . Shaded areas show values of  $\beta/k$  for which each approximation overestimates the full solution by less than 25%.

$$\frac{R}{kC_\infty} = \frac{\beta/k}{1 + \beta/k} \quad (8)$$

The dimensionless ratios in Eq. 8 may be readily interpreted.  $R/kC_\infty$ , the dimensionless uptake rate, is the ratio of the actual uptake rate to the maximum possible uptake rate.  $\beta/k$ , the dimensionless mass transfer coefficient, is the ratio of the mass transfer coefficient to the first-order uptake rate constant.

Eq. 8 is plotted in Fig. 1. It is well approximated by  $R/kC_\infty = \beta/k$  for  $\beta/k \ll 1$ , as shown by the dashed straight line asymptotic to the full solution curve on the left-hand side of the figure. Dimensionally, this is equivalent to  $R = \beta C_\infty$ , which is the expression for mass transfer controlled uptake (Frank-Kamenetskii 1969; Boudreau and Guinasso 1982; Bilger and Atkinson 1995). Uptake appears to be a first-order process, but the apparent reaction rate constant is a function of flow and is independent of the actual uptake kinetics at the boundary. On the other hand, Eq. 8 is well approximated by  $R/kC_\infty = 1$  for  $\beta/k \gg 1$ , as shown by the dashed horizontal line in Fig. 1. Dimensionally, this is equivalent to  $R = kC_\infty$ , which is the expression for kinetically controlled first-order uptake.

The intermediate region where both mass transfer and kinetics are important is quite broad with first-order kinetics, and both mass transfer control and kinetic control are poor approximations to the actual uptake rate in this region. For example, at  $\beta/k = 1$  both approximations are 100% overestimates of actual uptake rate. If we define an overestimation of no more than 25% as an acceptable criterion for the accuracy of the asymptotic approximations, then  $\beta/k < 0.25$  is the region of validity for mass transfer control and  $\beta/k > 4$  is the region of validity for kinetic control; these regions are shaded in Fig. 1.

There are a number of possible nondimensionalizations of

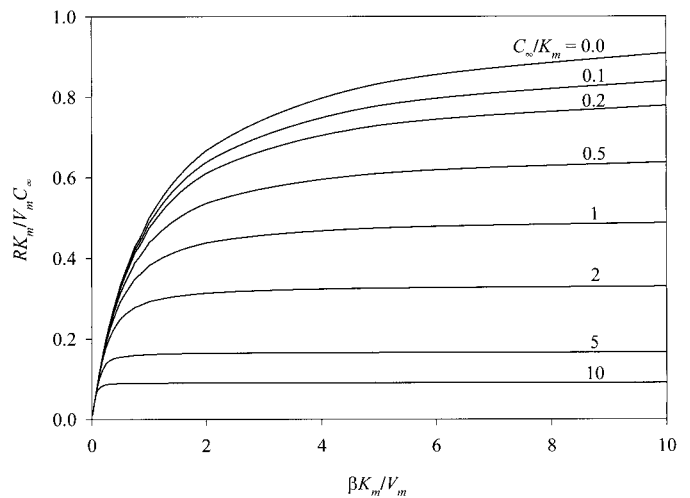


Fig. 2. Dimensionless uptake rate  $RK_m/V_m C_\infty$  plotted against dimensionless mass transfer coefficient  $\beta K_m/V_m$  for Monod kinetics (Eq. 10). Each curve represents the solution for a constant value of  $C_\infty/K_m$ .  $C_\infty/K_m = 0$  is identical to the first-order kinetics curve in Fig. 1.

Monod uptake, but the best one for comparison to the first-order case and for examination of the influence of mass transfer may be derived by dividing Eq. 6 by  $V_m C_\infty/K_m$ :

$$\frac{RK_m}{V_m C_\infty} = \frac{\frac{C_o}{C_\infty}}{1 + \frac{C_\infty C_o}{K_m C_\infty}} = \frac{\beta K_m}{V_m} \left( 1 - \frac{C_o}{C_\infty} \right) \quad (9)$$

Using the right-hand equality of Eq. 9 to eliminate  $C_\infty/C_o$  (algebraically simpler than eliminating  $C_o/C_\infty$  in this case) yields

$$\frac{RK_m}{V_m C_\infty} = \left[ \frac{C_\infty}{K_m} + \frac{1}{2} \left( \gamma + \sqrt{\gamma^2 + 4 \frac{C_\infty}{K_m}} \right) \right]^{-1} \quad (10)$$

where

$$\gamma = 1 + \left( \frac{\beta K_m}{V_m} \right)^{-1} - \frac{C_\infty}{K_m}$$

The dimensionless ratios in Eq. 10 also are easily interpreted. The dimensionless uptake rate  $RK_m/V_m C_\infty$  is analogous to  $R/kC_\infty$  in the first-order solution. It is the ratio of the actual uptake rate to the maximum possible uptake rate as  $C_\infty \rightarrow 0$ , where Monod kinetics behave like first-order kinetics with  $k \sim V_m/K_m$ . The dimensionless mass transfer coefficient  $\beta K_m/V_m$  is similarly analogous to  $\beta/k$  in the first-order solution. The dimensionless bulk concentration  $C_\infty/K_m$  has no analog in the first-order solution, but it is a good indicator of the degree of eutrophication relative to Monod saturation.

Eq. 10 is shown graphically in Fig. 2 as a family of curves, each with a different constant value of  $C_\infty/K_m$ , plotted against  $\beta K_m/V_m$ . Curves are plotted for  $C_\infty/K_m$  ranging from 0 through 10 (oligotrophic conditions) to 10 (eutrophic conditions). The solution for  $C_\infty/K_m = 0$  is identical to the first-order solution shown in Fig. 1, and it is an envelope for all

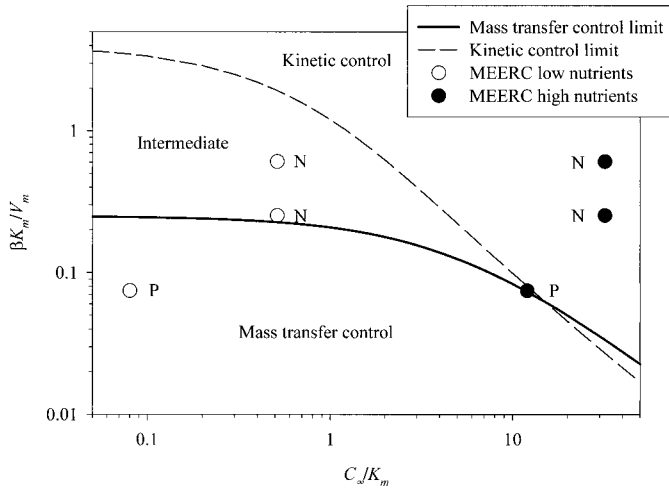


Fig. 3. Mass transfer and kinetic control limits of  $\beta K_m/V_m$  plotted against dimensionless concentration  $C_\infty/K_m$  for Monod kinetics. Limits are defined by the value of  $\beta K_m/V_m$  for which each approximation overestimates the full solution by 25% (Eqs. 12 and 13). MEERC data in Table 1 are plotted as well, for  $\text{NO}_3 + \text{NO}_2$  (N) and  $\text{PO}_4$  (P) uptake at low (open circles) and high (closed circles) ambient nutrient concentrations.

of the Monod solutions. Near  $\beta K_m/V_m = 0$ , the curves all approach  $RK_m/V_m C_\infty = \beta K_m/V_m$ . Just as in the first-order case, this is dimensionally equivalent to  $R = \beta C_\infty$ , and it represents mass transfer controlled uptake. As  $\beta K_m/V_m$  increases, uptake asymptotically tends toward kinetic control. Under increasingly eutrophic conditions, this happens at lower and lower values of  $\beta K_m/V_m$ . The level of each of the curves under kinetic control is given by

$$\left(\frac{RK_m}{V_m C_\infty}\right)_{\max} = \frac{1}{1 + \frac{C_\infty}{K_m}} \quad (11)$$

Following the line of reasoning introduced in the discussion of first-order kinetics, we define an overestimation of no more than 25% as an acceptable criterion for the accuracy of the mass transfer control approximation at low  $\beta K_m/V_m$  and the kinetic control approximation at high  $\beta K_m/V_m$ . These limits are given by

$$\frac{\beta K_m}{V_m} < \frac{0.25}{1 + 0.2 \frac{C_\infty}{K_m}} \quad (12)$$

for mass transfer control and

$$\frac{\beta K_m}{V_m} > \frac{4 + 0.8 \frac{C_\infty}{K_m}}{\left(1 + \frac{C_\infty}{K_m}\right)^2} \quad (13)$$

for kinetic control. They are plotted in Fig. 3. Examination of Eqs. 12 and 13 and Fig. 3 reveals that both limits become vanishingly small as  $C_\infty/K_m$  becomes very large. This means

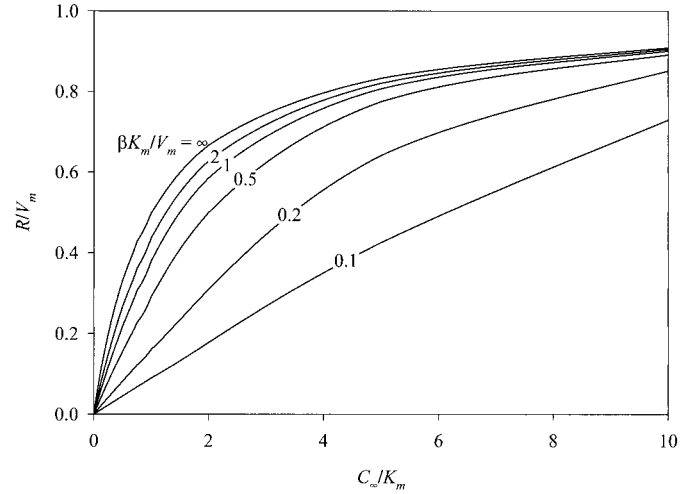


Fig. 4. Dimensionless uptake rate  $R/V_m$  plotted against dimensionless concentration  $C_\infty/K_m$  for Monod kinetics. Each curve represents the solution for a constant value of  $\beta K_m/V_m$ .  $\beta K_m/V_m = \infty$  is identical to the standard Monod kinetics expression (Eq. 4). As  $\beta K_m/V_m$  approaches zero, mass transfer controls uptake.

that under increasingly eutrophic conditions mass transfer control becomes less and less important, kinetic control becomes an increasingly good approximation, and the intermediate range becomes smaller and smaller. The limit curves cross at  $C_\infty/K_m = 15$ ; both approximate solutions overestimate by less than 25% in the overlap range for  $C_\infty/K_m > 15$ .

Another view of the effects of mass transfer limitation on uptake with Monod kinetics is presented in Fig. 4. This figure shows a family of curves of the nondimensional ratio  $R/V_m$ , each with a different constant value of  $\beta K_m/V_m$ , plotted against  $C_\infty/K_m$ . These solutions are derived simply by multiplying both sides of Eq. 10 by  $C_\infty/K_m$ . Curves are plotted for  $\beta K_m/V_m$  ranging from 0.1 (mass transfer control) to  $\infty$  (kinetic control). The solution for  $\beta K_m/V_m = \infty$  is identical to the standard Monod kinetic equation with  $C_\infty$  substituted for  $C_0$ . Curves such as those in Fig. 4 might be generated from experimental data on uptake rate versus concentration, with the different curves representing different flow conditions. Fig. 4 indicates that mass transfer limitation should have little practical effect on derived kinetic parameters for  $\beta K_m/V_m > 2$ . As  $\beta K_m/V_m$  decreases below 2, mass transfer begins to limit uptake, resulting in marked deviations of the uptake rate curve from pure Monod kinetics. Estimates of kinetic parameters obtained with  $\beta K_m/V_m < 2$  thus might be erroneous, especially for low values of  $C_\infty/K_m$ . At low  $C_\infty/K_m$  and  $\beta K_m/V_m \approx 0.1$ , the curves approach straight lines with slopes approximated by the value of  $\beta K_m/V_m$ . Under these conditions an uptake kinetics experiment ignoring mass transfer effects might lead to the mistaken conclusion that uptake kinetics were first-order, when in fact uptake was mass transfer controlled with Monod kinetics.

Finally, we should note the similarity between the solution shown in Fig. 4 and solutions presented by Pasciak and Gavis (1974) and Wheeler (1980), among others. Pasciak and Gavis derived a dimensionless transport ratio  $P$ , very similar to our  $\beta K_m/V_m$ , which depends on shape, radius, and settling

or swimming speed of phytoplankton at very low Reynolds numbers instead of our mass transport velocity. They suggested that  $P < 2$  implies transport limitation, in accordance with our discussion above. Wheeler (1980) considered the interaction between flow and fixation of carbon by giant kelp leaves; he presented data and calculations that are similar to Fig. 4 and one experimental plot reminiscent of Fig. 2. These previous formulations were for specific problems, and their results were therefore somewhat less general than ours. More importantly, they did not consider the interaction between mass transfer limitation and bulk concentration. It would be interesting to reconsider their results in light of the concentration dependence predicted here.

*Example calculations*—The approach we have developed here allows direct theoretical prediction of the influence of mass transfer on uptake, given reasonable estimates of the controlling parameters. These parameter estimates must include the mass transfer velocity (or its components), the controlling kinetic parameters, and the bulk fluid concentration. In the following, we present and discuss example calculations using data on uptake kinetics and boundary shear velocities from wall and benthic flux measurements in experimental ecosystem tanks.

Incubation experiments were run using wall strips and sediments from experimental ecosystem enclosures [the Multiscale Experimental Ecosystem Research Center (MEERC) Pelagic/Benthic tanks at the University of Maryland Center for Environmental Science, Horn Point Laboratory] to measure the parameters controlling uptake of nutrients at the wall and bottom boundaries (C.-C. Chen and E. Porter, pers. comm.). These experiments were run in separate, well-mixed incubation chambers and are assumed not to have been affected by mass transfer limitation, such that the derived kinetic parameters are reasonable estimates of the true kinetic parameters of the wall and benthic communities. Monod parameters were estimated using Lineweaver-Burk plots (Fogler 1992) to fit the observed data. Resultant estimates of  $V_m/K_m$  were  $0.01 \text{ m h}^{-1}$  for  $\text{NO}_3 + \text{NO}_2$  at the bottom boundary and  $0.45 \text{ m h}^{-1}$  for  $\text{PO}_4$  at the wall boundary, based on experiments with highly significant Lineweaver-Burk regressions ( $r^2 = 0.95$ ,  $p < 0.05$  for  $\text{NO}_3 + \text{NO}_2$  and  $r^2 = 0.85$ ,  $p < 0.05$  for  $\text{PO}_4$ ). Corresponding estimates of  $K_m$  were  $1.56 \mu\text{M}$  for  $\text{NO}_3 + \text{NO}_2$  and  $0.25 \mu\text{M}$  for  $\text{PO}_4$ .

Estimates of wall and bottom shear velocities in the MEERC P/B tanks were obtained separately using hot film sensors (Crawford and Sanford pers. comm.) at a number of different mixing rates. The  $u_*$ s at the standard mixing rates for MEERC experiments fall into two distinct groups. Average shear velocities at the bottom boundary of the large ( $10 \text{ m}^3$ ) tanks were significantly lower ( $0.05 \text{ cm s}^{-1}$ ) than average shear velocities at the bottoms of the smaller tanks and at the walls of all of the tanks ( $0.12 \text{ cm s}^{-1}$ ). The boundary layers on the walls and bottoms of the tanks were all smooth turbulent. The Schmidt numbers of  $\text{NO}_3$  and  $\text{NO}_2$  are very similar at  $22^\circ\text{C}$  and a salinity of 14, averaging 600, whereas the Schmidt number of  $\text{PO}_4$  under these conditions is 1,440. Substituting these values into Eq. 2 yields three different estimates for  $\beta$ :  $0.0061 \text{ m h}^{-1}$  for  $\text{NO}_3 + \text{NO}_2$  at  $u_* = 0.12 \text{ cm s}^{-1}$ ,  $0.0034 \text{ m h}^{-1}$  for  $\text{PO}_4$  at  $u_* = 0.12 \text{ cm}$

$\text{s}^{-1}$ , and  $0.0025 \text{ m h}^{-1}$  for  $\text{NO}_3 + \text{NO}_2$  at  $u_* = 0.05 \text{ cm s}^{-1}$ . We do not list  $\beta$  for  $\text{PO}_4$  at  $u_* = 0.05 \text{ cm s}^{-1}$  because no estimates of kinetic parameters for  $\text{PO}_4$  were available at the bottom boundary of the large tanks.

Water column concentrations of  $\text{NO}_3 + \text{NO}_2$  and  $\text{PO}_4$  varied significantly over the course of most MEERC P/B experiments, but broadly speaking they could be classified as high or low. Experiments were initiated with ambient Choptank River water, which in the summer and fall tended to have relatively low concentrations of  $\text{NO}_3 + \text{NO}_2$  and  $\text{PO}_4$ . After an initial adjustment period of approximately 1 week, a nutrient pulse was applied, increasing water column  $\text{NO}_3 + \text{NO}_2$  and  $\text{PO}_4$  concentrations by approximately 2 orders of magnitude. Concentrations decreased rapidly following the nutrient pulse as the nutrients were assimilated. A significant fraction of total nutrient uptake occurred at the walls and benthos of the tanks (Chen et al. 1997). A typical low  $\text{NO}_3 + \text{NO}_2$  concentration was  $0.8 \mu\text{M}$ , and a typical low  $\text{PO}_4$  concentration was  $0.02 \mu\text{M}$ . Immediately after the nutrient pulse,  $\text{NO}_3 + \text{NO}_2$  concentration was elevated to  $50 \mu\text{M}$  and  $\text{PO}_4$  concentration to  $3 \mu\text{M}$  (Petersen et al. 1997).

The above estimates of  $\beta$ ,  $V_m/K_m$ ,  $K_m$ , and  $C_\infty$  for summertime MEERC P/B experiments are summarized in Table 1. All of these estimated values are approximate, but they are more than adequate for our purposes. They were used to calculate  $\beta K_m/V_m$ ,  $C_\infty/K_m$ , the mass transfer control limit ( $\text{MT}_{\text{lim}}$ , Eq. 12), and the kinetic control limit ( $\text{K}_{\text{lim}}$ , Eq. 13), and the results are listed in Table 1 and shown graphically in Fig. 3. Comparison of  $\beta K_m/V_m$  to  $\text{MT}_{\text{lim}}$  and  $\text{K}_{\text{lim}}$  allows estimation of the degree of mass transfer limitation of boundary uptake under different conditions in the MEERC P/B tanks. Under low nutrient conditions, nutrient uptake was either mass transfer controlled or only slightly into the intermediate range. Mass transfer control was most pronounced for  $\text{PO}_4$  uptake because its relatively high value of  $V_m/K_m$  ensured that  $\beta K_m/V_m$  was always low. The influence of flow is apparent when comparing low  $u_*$  to high  $u_*$  estimates for  $\text{NO}_3 + \text{NO}_2$  uptake. Low  $u_*$   $\text{NO}_3 + \text{NO}_2$  uptake was very close to mass transfer control, whereas high  $u_*$  was intermediate between mass transfer control and kinetic control. In any case, under relatively oligotrophic conditions nutrient uptake was always primarily controlled by flow, and uptake kinetics played only a secondary role.

Under high nutrient conditions, with  $C_\infty$  increased by approximately 2 orders of magnitude, the environment was changed from oligotrophic to eutrophic relative to wall and bottom uptake kinetics. The limit values for mass transfer and kinetic control are both significantly smaller at these high concentrations, such that all  $\text{NO}_3 + \text{NO}_2$  uptake was strongly kinetically controlled and  $\text{PO}_4$  uptake was intermediate between mass transfer control and kinetic control. Under these conditions flow likely had little effect on uptake, which was primarily controlled by the kinetics of nutrient use by the wall and bottom communities.

The calculations described here allow direct estimation of the influence of mass transfer on boundary uptake, but there are several uncertainties inherent in the parameter estimates needed for these calculations. One important uncertainty is the possibility that the procedures used to estimate the kinetic parameters may themselves have been subject to mass

Table 1. Example estimates of mass transfer (*MT*) versus kinetic (*K*) control of  $\text{NO}_3 + \text{NO}_2$  (N) and  $\text{PO}_4$  (P) uptake at the walls and benthos of the MEERC mesocosms; *I* = intermediate between *MT* and *K* control. Data sources described in text.

$\mu_{\text{N}}^*$ ( $\text{cm s}^{-1}$ )	Nutrient conditions	$\beta$ ( $\text{m h}^{-1}$ )	$V_m/K_m$ ( $\text{m h}^{-1}$ )	$K_m$ ( $\mu\text{M}$ )	$C_{\infty}$ ( $\mu\text{M}$ )	$C_{\infty}/K_m$	$\beta K_m/V_m$	<i>MT</i> <sub>lim</sub>	$K_{\text{lim}}$	Control
0.12	low N	0.0061	0.01	1.56	0.8	0.51	0.61	0.23	1.93	<i>I</i>
	high N	0.0061	0.01	1.56	50	32.05	0.61	0.03	0.03	<i>K</i>
	low P	0.0034	0.45	0.25	0.02	0.08	0.07	0.25	3.48	<i>MT</i>
	high P	0.0034	0.45	0.25	3.0	12.00	0.07	0.07	0.08	<i>I</i>
0.05	low N	0.0025	0.01	1.56	0.8	0.51	0.25	0.23	1.93	<i>I</i>
	high N	0.0025	0.01	1.56	50	32.05	0.25	0.03	0.03	<i>K</i>

transfer limitation. We assumed this was not a problem for the present calculations because the uptake experiments were well mixed and because our primary emphasis is on illustrating the calculation procedure rather than determining definitive parameter values. In any case, this uncertainty is likely to affect  $K_m$  estimates more than  $V_m$  estimates. Referring to Figs. 3 and 4, it is apparent that as long as  $C_{\infty}/K_m$  is high and there is modest flow energy, estimates of  $V_m$  should not be affected significantly by mass transfer limitation. Under the oligotrophic conditions needed to determine the shape of an uptake curve near  $C_{\infty}/K_m = 0$ , however, mass transfer limitation is much more likely. Mass transfer limitation decreases the slope of the uptake curve in this region (Fig. 4), which leads to an underestimate of  $V_m/K_m$ . This in turn leads to an overestimate of  $K_m$ , assuming a trustworthy estimate of  $V_m$ . An overestimate of  $K_m$  means an underestimate of  $C_{\infty}/K_m$  and an overestimate of  $\beta K_m/V_m$ . This translates to a bias upward and toward the left in Fig. 3, which may or may not result in a misdiagnosis of the relative influences of mass transfer and kinetics.

Possible solutions to this problem include using Eq. 10 to correct the kinetic parameter estimates (a complex iterative procedure) or simply assuming a reasonable value for overestimation of  $K_m$  in order to estimate potential errors. However, a better solution is to derive kinetic parameters from uptake experiments not affected by mass transfer limitation in the first place. For example, one might begin uptake experiments at a low concentration with gentle mixing, increase mixing until there is no further increase in uptake, then maintain that mixing rate as concentration is increased until uptake saturates. This would yield both reasonable estimates of the true kinetic parameters and an indication of the behavior of the mass transfer coefficient in the experimental apparatus.

Determining or predicting the mass transfer coefficient  $\beta$  is the other potential major uncertainty in these calculations. We have assumed that  $\beta$  is known, but we do not mean to imply that determining  $\beta$  is trivial. This often requires careful experimentation with particular attention to replication of flow conditions likely to be encountered in nature. A full discussion of the factors that control the mass transfer coefficient is beyond the scope of this paper, but see, e.g., Bilger and Atkinson (1992), Patterson (1992), Dade (1993), or Ploug et al. (1999).

In conclusion, both the theory and the examples presented here reinforce the importance of considering all of the factors that affect boundary uptake, not just mass transfer and not just kinetics. Mass transfer control is more likely in low-energy, oligotrophic environments for uptake kinetics characterized by high ratios of  $V_m/K_m$  (or high first-order reaction rate coefficients). Kinetic control is more likely in high-energy, eutrophic environments for uptake kinetics characterized by low ratios of  $V_m/K_m$  (or low first-order reaction rate coefficients). However, there are many situations in which both mass transfer and kinetics are important, when a change in any of the controlling parameters can affect boundary uptake significantly.

Lawrence P. Sanford<sup>1</sup>  
Sean M. Crawford

University of Maryland Center for Environmental Science  
Horn Point Laboratory  
P.O. Box 775, Cambridge, Maryland 21613

### References

- ATKINSON, B., AND I. J. DAVIES. 1974. The overall rate of substrate uptake (reaction) by microbiofilms. Part I—a biological rate equation. *Inst. Chem. Eng. Trans.* **52**: 248–259.
- ATKINSON, M. J. AND R. W. BILGER. 1992. Effects of water velocity on phosphate uptake in coral reef-flat communities. *Limnol. Oceanogr.* **37**: 273–279.
- BAIRD, M. E., AND M. J. ATKINSON. 1997. Measurement and prediction of mass transfer to experimental coral reef communities. *Limnol. Oceanogr.* **42**: 1685–1693.
- BILGER, R. W., AND M. J. ATKINSON. 1992. Anomalous mass transfer of phosphate on coral reef flats. *Limnol. Oceanogr.* **37**: 261–272.
- , AND ———. 1995. Effects of nutrient loading on mass-transfer rates to a coral-reef community. *Limnol. Oceanogr.* **40**: 279–289.
- BOUDREAU, B. P., AND N. L. GUINASSO. 1982. The influence of a diffusive sublayer on accretion, dissolution, and diagenesis at the seafloor, p. 115–145. *In* K. A. Fanning and F. T. Manheim [eds.], *The dynamic environment of the ocean floor*. D.C. Heath.
- , AND M. R. SCOTT. 1978. A model for the diffusion-controlled growth of deep-sea manganese nodules. *Am. J. Sci.* **278**: 903–929.
- CHEN, C.-C., J. E. PETERSEN, AND W. M. KEMP. 1997. Spatial and temporal scaling of periphyton growth on walls of estuarine mesocosms. *Mar. Ecol. Prog. Ser.* **155**: 1–15.
- , K. P. SEBENS, AND R. R. OLSON. 1991. In situ measurements of flow effects on primary production and dark respiration in reef corals. *Limnol. Oceanogr.* **36**: 936–948.
- PETERSEN, J. E., C. C. CHEN, AND W. M. KEMP. 1997. Scaling aquatic primary productivity: Experiments under nutrient- and light-limited conditions. *Ecology* **78**: 2326–2338.
- PLOUG, H., W. STOLTE, AND B. B. JØRGENSEN. 1999. Diffusive boundary layers of the colony-forming plankton alga *Phaeocystis* sp.—implications for nutrient uptake and cellular growth. *Limnol. Oceanogr.* **44**: 1959–1967.
- RIBER, H. H., AND R. G. WETZEL. 1987. Boundary layer and internal diffusion effects on phosphorus fluxes in lake periphyton. *Limnol. Oceanogr.* **32**: 1181–1194.
- SANTSCHI, P. H., R. F. ANDERSON, M. Q. FLEISHER, AND W. BOWLES. 1991. Measurements of diffusive sublayer thicknesses in the ocean by alabaster dissolution, and their implications for the measurements of benthic fluxes. *J. Geophys. Res.* **96**: 10,641–10,657.
- , P. HOHENER, G. BENOIT, AND M. BUCHHOLTZ-TEN BRINK. 1990. Chemical processes at the sediment-water interface. *Mar. Chem.* **30**: 269–315.
- THOMAS, F. I. M., AND M. J. ATKINSON. 1997. Ammonium uptake by coral reefs: Effects of water velocity and surface roughness on mass transfer. *Limnol. Oceanogr.* **42**: 81–88.
- WHEELER, W. N. 1980. Effect of boundary layer transport on the fixation of carbon by the giant kelp *Macrocystis pyrifera*. *Mar. Biol.* **56**: 103–110.
- DADE, W. P. 1993. Near-bed turbulence and hydrodynamic control of diffusional mass transfer at the sea floor. *Limnol. Oceanogr.* **38**: 52–69.
- FOGLER, H. S. 1992. *Elements of chemical reaction engineering*. 2nd ed. Prentice Hall.
- FRANK-KAMENETSKII, D. A. 1969. *Diffusion and heat transfer in chemical kinetics*. Plenum.
- JØRGENSEN, B. B., AND N. P. REVSBECH. 1985. Diffusive boundary layers and the oxygen uptake of sediments and detritus. *Limnol. Oceanogr.* **30**: 111–122.
- KOCH, E. W. 1994. Hydrodynamics, diffusion-boundary layers and photosynthesis of the seagrasses *Thalassia testudinum* and *Cymodocea nodosa*. *Mar. Biol.* **118**: 767–776.
- PASCIAK, W. J., AND J. GAVIS. 1974. Transport limitation of nutrient uptake in phytoplankton. *Limnol. Oceanogr.* **19**: 881–888.
- PATTERSON, M. R. 1992. A chemical engineering view of cnidarian symbioses. *Am. Zool.* **32**(4): 566–582.

Received: 4 January 1999  
Amended: 17 April 2000  
Accepted: 24 April 2000

<sup>1</sup> Corresponding author (lsanford@hpl.umces.edu).

### Acknowledgements

The authors gratefully acknowledge C.-C. Chen and E. Porter for giving us access to their data, and we thank E. Koch, J. Cornwell, M. L. Chang, and four anonymous reviewers for their helpful comments on earlier versions of this manuscript. This research was supported by the USEPA STAR program as part of the Multiscale Experimental Ecosystem Research Center (MEERC) at the University of Maryland Center for Environmental Science (UMCES) through grant number R 819640. UMCES publication number 3311.